Experimental study of upward-going muons in Kamiokande

Y. Oyama, K. S. Hirata, T. Kajita, T. Kifune, K. Kihara, M. Nakahata,
K. Nakamura, S. Ohara, N. Sato, M. Takita, Y. Totsuka, and Y. Yaginuma

Institute for Cosmic Ray Research, University of Tokyo, Tokyo 188, Japan

M. Mori, A. Suzuki, K. Takahashi, T. Tanimori, and M. Yamada

National Laboratory for High Energy Physics (KEK), Ibaraki 305, Japan

M. Koshiba

Department of Physics, Faculty of Science, Tokai University, Kanagawa 259-12, Japan

T. Suda

Department of Physics, Faculty of Science, Kobe University, Hyogo 657, Japan

K. Miyano, H. Miyata, and H. Takei

Department of Physics, Niigata University, Niigata 950-21 Japan

K. Kaneyuki, Y. Nagashima, and Y. Suzuki

Department of Physics, Osaka University, Osaka 560, Japan

E. W. Beier, L. R. Feldscher, E. D. Frank, W. Frati, S. B. Kim, A. K. Mann,
F. M. Newcomer, R. Van Berg, and W. Zhang

Department of Physics, University of Pennsylvania, Philadelphia, Pennsylvania 19104

(Received 29 September 1988)

Upward-going muons produced in the surrounding rock by high-energy neutrinos from astronomical objects have been searched for using the large underground water Cherenkov detector, Kamiokande. During a total of 1255 days observation, no significant signal was observed from the direction of eight astronomical objects. The 90%-confidence-level (-C.L.) upper limits on upward-going muon fluxes with energy greater than 1.7 GeV are 9.9×10^{-14} cm^{-2}s^{-1} for Cygnus X-3 and 2.6×10^{-14} cm^{-2}s^{-1} for LMC X-4. Our observed upward-going muon flux is compared with the calculation of the upward-going muon flux produced by the atmospheric neutrinos to examine the neutrino-oscillation hypothesis. The experimental average upward-going muon flux with energy greater than 1.7 GeV, $(2.05\pm0.18)\times10^{-13}$ cm^{-2}s^{-1}sr^{-1}, is consistent with the theoretical expectation. If $\nu_\mu \leftrightarrow \nu_\tau$ vacuum oscillations and large mixing angle are assumed, $\Delta m^2 \gtrsim 10^{-2}$ eV^2 is newly rejected. The 90%-C.L. upper limit on the Δm^2 for the maximum mixing is found to be $\Delta m^2 = 0.03$ eV^2 and $\Delta m^2 = 0.0055$ eV^2, depending on assumptions.

I. INTRODUCTION

High-energy muon neutrinos, which are observed as upward-going muons in deep-underground detectors, are interesting objects in both astrophysics and particle physics. From the viewpoint of astrophysics, neutrinos are a good probe to study astronomical objects because they are neutral and quite stable particles. Since neutrinos can relatively easily penetrate matter, they can provide information on the interior of astronomical objects or objects behind galactic clouds which are not observable by means of photons. High-energy neutrinos are a possible clue to understand the acceleration mechanism of cosmic-ray protons for the following reason. The time-dependent strong magnetic field of neutron stars is thought to accelerate cosmic-ray protons. Accelerated protons themselves are not useful in astronomy because they are diffused in the interstellar magnetic field and lose their

directions. On the other hand, if matter exists near the neutron star, pions would be produced by nuclear interactions between the accelerated protons and the matter. Muon neutrinos, which are decay products of charged pions, are expected to be generated together with γ rays from neutral pions. These neutrinos and γ rays would be observable in directional astronomy because they are stable and do not lose their directions. This condition, i.e., neutron star and nearby matter, is realized when a neutron star is accompanied by a comparison star,[1] or when a neutron star just after supernova explosion is surrounded by the thick gas which initially comprised the envelope of the progenitor, and later became dispersed by the supernova explosions.[2] In a previous paper,[3] we presented the result of a search for supernova high-energy neutrinos using the excellent opportunity arranged by SN 1987A. In this paper, we report the result of a search related to the observations of VHE (very high energy, 10^{12} eV) and UHE (ultrahigh energy, 10^{15} eV) γ-ray sources such as Cygnus X-3 (Ref. 4) or LMC X-4 (Ref. 5).

In this extraterrestrial neutrino search, the main background is upward-going muons produced by atmospheric neutrinos from the opposite side of Earth. From the viewpoint of particle physics, the atmospheric neutrinos are a probe to search for neutrino oscillations.[6] If two-neutrino mixing is assumed, the probability that ν_x with energy E (GeV) remains ν_x after traveling a distance L (km) in the vacuum is

$$P(\nu_x \rightarrow \nu_x) = 1 - \sin^2 2\theta \sin^2 \left[1.27 \times \frac{L \Delta m^2}{E} \right], \quad (1)$$

where Δm^2 (eV^2) is the difference of squared masses of two neutrinos and θ is the mixing angle. Because atmospheric neutrinos generated at the opposite side of Earth travel possibly the longest distance in terrestrial experiments, the flux of upward-going muons may be affected by neutrino oscillations. It is possible to investigate whether or not neutrinos oscillate up to $\Delta m^2 = 10^{-2} - 10^{-3}$ eV^2 by comparing the observed upward-going muon flux with the expected one. In the case of $\nu_e \leftrightarrow \nu_\mu$ oscillation, the matter effect due to penetration of Earth must in general be taken into account.[7] However, the difference between matter and vacuum oscillations is small because the energy of the neutrinos considered here is much higher than that of, for example, the solar neutrinos, in which case the neutrino flux might be affected drastically. In this paper, together with a search for astronomical extraterrestrial neutrino sources, a comparison is made between the upward-going muon flux in Kamiokande and the flux obtained by calculation of the atmospheric neutrino products to test the neutrino-oscillation hypothesis.

II. MUONS FROM ASTRONOMICAL OBJECTS

Kamiokande (Kamiokande-I and its upgraded phase, Kamiokande-II) is an imaging water Cherenkov detector located 2700 m.w.e. (meters of water equivalent) underground in the Kamioka mine, about 300 km west of Tokyo (36.42°N, 137.31°E). In Kamiokande-I, 2340 tons of water in a cylindrical steel tank are viewed by 1000 20-inch photomultiplier tubes (PMT's) covering 20% of the tank surface. In Kamiokande-II, the inner detector is surrounded by a 4π anticounter layer which contains at least 1.5-m-thick water, viewed by 123 20-in. PMT's. In order to construct the bottom anticounter, the volume and number of PMT's in the inner counter were reduced to be 2140 tons and 948, respectively. A more detailed description of Kamiokande is given in Ref. 8 (Kam-I) and Refs. 9 and 10 (Kam-II).

Data from the time period between July 6, 1983 and March 14, 1988 are analyzed. They correspond to 844 days of "weekday data" which are fully efficient for upward-going muons and 411 days of "holiday data" in which 50% of upward-going muons are not recorded. A total of 6.04×10^7 events have been recorded during this period. Two independent algorithms were used to select upward-going muons from the raw data. The selection efficiency was 97%. After selection, 60 488 events survived, almost all of which are downward-going muons traveling almost horizontally, or multiple muons. Upward-going muons are picked up by two independent visual scans, and are reconstructed manually. A total of 146 upward-going muons (zenith angle larger than 90°, path length ≥ 7 m, corresponding to an energy threshold of 1.7 GeV) are selected from the nominal area of 165 m^2 (Kam-I) and 150 m^2 (Kam-II). The effective area of the detector as a function of zenith angle is shown in Fig. 1. A complete list of upward-going muons is presented in Table I.

Figure 2 shows a horizontal distribution of upward-going muons. Downward-going muons which were produced in the upper atmosphere and traveling almost horizontally are also plotted. Downward-going muons cannot reach the detector from zenith angle larger than $\sim 86°$ because of a large rock overburden in the horizontal direction. Actually, in Fig. 2, upward-going muons
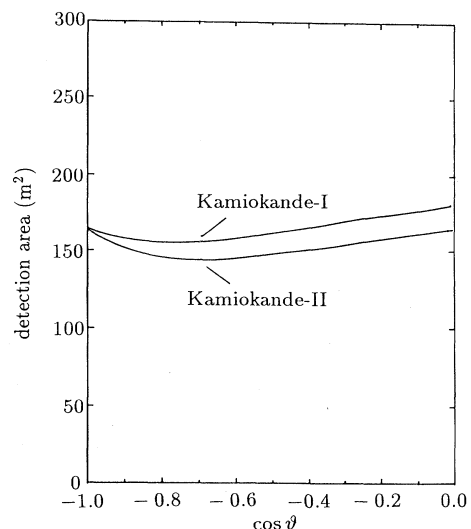
FIG. 1. The detection area as a function of zenith angle. Nominal detection areas are 165 and 150 m^2 for Kamiokande-I and Kamiokande-II, respectively.

TABLE I. A list of 146 upward-going muons. Observation times, arrival directions in the horizontal coordinate and in the celestial coordinate are presented. The observation times are given by UT (universal time). The azimuth angle is defined such that 0° and 90° correspond to south and west, respectively. The temporal variation in the number of upward-going muons is due to live time.

	Run	Event	Date	Time	Azim. (deg)	Zeni. (deg)	R.A. (deg)	Decl. (deg)
1	73	1 309	83-07-16	00:13:56	232.7	−11.4	197.3	21.2
2	82	3 563	83-07-21	09:56:59	62.3	−25.7	128.0	−36.5
3	102	23 011	83-08-01	22:07:45	217.2	−18.9	200.3	24.5
4	121	5 832	83-08-18	10:39:12	239.6	−33.0	37.0	1.0
5	160	1 117	83-09-13	6:50:36	227.4	−24.5	8.0	14.4
6	188	18 771	83-09-30	20:06:49	25.8	−6.7	43.4	−52.1
7	193	5 674	83-10-04	02:41:42	43.5	−0.9	131.2	−36.4
8	235	32 414	83-10-29	21:30:40	57.3	−81.1	327.5	−40.8
9	244	7 510	83-11-07	12:06:22	102.1	−22.9	249.6	−4.3
10	259	28 758	83-11-14	21:08:14	110.3	−54.9	2.5	−19.0
11	300	21 159	83-12-16	19:41:28	353.1	−75.8	334.9	−50.4
12	336	8 731	84-01-13	13:05:08	52.8	−10.5	10.6	−35.9
13	371	3 997	84-02-06	02:26:26	266.9	−14.1	52.5	−5.9
14	384	17 904	84-02-14	18:13:44	182.8	−69.2	13.7	−15.6
15	407	4 551	84-02-27	10:21:53	178.2	−11.9	271.6	41.6
16	419	20 746	84-03-03	18:40:59	181.2	−41.7	38.4	11.9
17	463	11 653	84-04-06	05:39:07	119.0	−1.1	307.6	22.2
18	478	10 904	84-04-17	05:51:03	355.0	−3.1	79.6	−56.4
19	480	1 014	84-04-17	23:54:17	181.5	−39.1	160.9	14.5
20	483	13 766	84-04-18	19:11:10	70.3	−0.5	193.8	−16.0
21	504	17 009	84-05-06	17:12:46	336.2	−9.7	305.0	−55.7
22	523	1 775	84-05-17	08:31:54	81.6	−34.8	25.0	−25.8
23	560	9 503	84-06-11	13:19:51	64.9	−12.5	151.9	−27.5
24	568	26 453	84-06-15	22:01:12	245.0	−24.4	136.2	3.6
25	574	20 329	84-06-20	19:45:14	18.2	−17.8	297.2	−65.5
26	592	16 821	84-06-28	18:03:21	212.2	−15.8	109.0	29.6
27	596	8 215	84-06-30	12:33:22	150.1	−39.9	87.2	8.9
28	657	23 526	84-08-2	21:02:46	39.9	−20.8	327.8	−52.0
29	723	8 905	84-09-11	13:01:22	217.5	−23.6	106.8	20.3
30	727	18 660	84-09-13	19:17:37	168.5	−14.7	253.8	37.7
31	728	1 342	84-09-14	00:38:10	59.1	−22.1	48.6	−37.3
32	769	4 902	84-09-27	100:16:29	56.4	−5.4	224.7	−30.0
33	862	27 025	85-03-7	13:35:27	81.5	−12.9	50.8	−14.4
34	884	68 004	85-04-1	19:02:46	315.1	−25.4	340.0	−50.4
35	915	19 081	85-04-17	16:54:41	335.9	−4.7	277.4	−51.4
36	916	2 016	85-04-18	13:00:49	49.9	−46.4	57.9	−51.9
37	920	31 033	85-04-22	21:55:05	149.3	−8.1	176.2	37.0
38	951	18 693	85-05-11	18:35:56	329.3	−42.3	39.3	−65.7
39	960	20 337	85-05-16	19:59:20	201.6	−5.5	101.3	43.4
40	1018	2 264	85-06-11	09:18:33	148.6	−6.0	37.9	38.4
41	1032	14 121	85-06-19	17:21:52	94.7	−61.1	159.1	−29.2
42	1060	5 173	85-07-08	11:05:00	118.8	−22.5	104.7	7.6
43	1077	3 032	85-07-22	09:07:23	222.8	−22.2	352.6	18.8
44	1117	7 381	85-08-09	02:00:46	316.1	−12.7	195.5	−44.2
45	1130	5 311	85-08-20	03:23:29	89.6	−55.4	17.2	−29.5
46	1158	3 971	85-09-05	01:38:54	111.3	−50.0	4.6	−15.5
47	1159	548	85-09-05	05:59:05	153.2	−64.6	42.8	−13.1
48	1168	5 058	85-09-10	04:44:12	9.3	−7.4	178.9	−59.8
49	1170	3 407	85-09-11	03:37:52	326.1	−3.7	233.5	−44.8
50	1174	25 336	85-09-12	22:42:22	220.2	−16.2	246.6	25.1
51	1183	8 016	85-09-18	12:03:48	229.9	−24.4	89.9	13.1
52	1183	12 171	85-09-18	14:19:56	47.0	−27.5	258.7	−49.5
53	1210	5 885	85-10-17	05:27:45	187.5	−70.0	62.3	−16.5
54	1211	6 050	85-10-17	11:15:48	179.2	−38.5	152.8	15.1
55	1212	1 528	85-10-18	01:23:15	270.0	−2.2	276.3	−1.3
56	1223	2 375	85-10-24	08:20:25	310.3	−8.0	5.6	−36.7

Y. OYAMA *et al.*

TABLE I. (*Continued*).

	Run	Event	Date	Time	Azim. (deg)	Zeni. (deg)	R.A. (deg)	Decl. (deg)
57	1325	11 675	86-01-09	05:12:38	30.3	−40.6	214.5	−66.0
58	1386	35 441	86-02-06	18:41:11	202.6	−31.9	354.1	18.5
59	1402	3 100	86-02-17	03:21:09	197.5	−16.9	134.1	34.2
60	1416	7 702	86-02-24	02:27:10	77.8	−8.0	238.6	−14.5
61	1450	31 963	86-03-13	19:48:13	92.8	−4.6	150.1	−0.5
62	1464	31 057	86-03-19	18:49:44	280.2	−28.2	345.1	−24.0
63	1473	2 799	86-03-31	07:27:29	33.0	−28.1	354.6	−61.0
64	1475	6 487	86-04-01	09:41:14	120.1	−33.7	338.1	0.3
65	1548	16 544	86-05-29	11:42:55	239.8	−26.1	328.5	5.8
66	1613	5 034	86-07-01	01:22:49	102.5	−1.3	338.3	9.2
67	1615	42 495	86-07-01	12:44:18	275.3	−69.3	42.0	−35.6
68	1624	28 627	86-07-07	02:53:56	119.3	−5.4	352.8	19.6
69	1684	151 289	86-08-21	03:55:58	62.7	−4.6	88.7	−24.5
70	1699	53 115	86-09-05	12:12:56	66.4	−8.2	222.4	−23.8
71	1707	128 096	86-09-11	19:34:57	7.3	−0.9	49.1	−53.9
72	1734	57 167	86-09-30	18:43:44	301.7	−67.8	220.3	−45.2
73	1740	63 299	86-10-06	22:01:12	186.8	−10.2	293.7	43.0
74	1749	34 326	86-10-13	08:52:04	86.0	−57.6	151.1	−32.1
75	1756	92 743	86-10-17	09:41:48	231.8	−8.2	69.9	24.1
76	1782	61 786	86-11-06	19:49:47	42.1	−49.1	354.4	−57.1
77	1795	241 211	86-11-16	20:00:27	320.0	−52.1	265.2	−58.4
78	1804	31 898	86-11-24	09:26:56	180.0	−13.3	162.2	40.3
79	1816	54 097	86-12-04	13:35:55	325.7	−18.4	122.9	−54.9
80	1827	62 349	86-12-15	19:51:56	147.9	−9.5	19.3	35.1
81	1841	62 990	86-12-26	00:50:16	347.3	−11.9	272.4	−63.0
82	1853	24 422	87-01-13	10:22:33	290.1	−37.3	158.9	−35.4
83	1868	28 169	87-01-30	12:35:35	336.5	−5.0	135.5	−51.8
84	1868	54 708	87-01-30	22:40:03	241.8	−36.0	21.4	−2.3
85	1884	23 383	87-02-14	12:25:23	337.1	−12.4	154.1	−58.3
86	1884	32 889	87-02-14	15:16:32	300.1	−18.9	239.0	−35.1
87	1890	33 769	87-02-20	18:16:43	10.7	−17.7	172.0	−69.0
88	1901	11 566	87-03-01	19:35:26	32.8	−29.9	144.0	−61.9
89	1905	54 512	87-03-06	02:11:51	221.6	−82.2	147.6	−30.4
90	1926	76 258	87-03-30	23:39:35	295.0	−8.4	41.8	−25.1
91	1958	29 575	87-05-05	05:20:31	103.6	−12.9	331.6	3.0
92	1959	23 882	87-05-06	08:03:12	151.8	−18.3	332.7	29.2
93	1963	36 063	87-05-09	16:15:08	117.9	−14.5	129.2	12.5
94	1971	3 744	87-05-16	02:29:15	44.8	−54.0	273.7	−54.7
95	1975	44 922	87-05-22	15:11:53	243.4	−25.0	10.6	4.4
96	1976	127 722	87-05-24	09:22:50	277.9	−43.9	284.5	−29.4
97	1981	37 789	87-05-29	18:33:27	71.5	−52.6	170.1	−38.8
98	1985	31 460	87-06-02	15:08:25	149.1	−28.6	103.4	18.7
99	1990	34 988	87-06-06	20:40:44	1.3	−70.6	163.0	−55.8
100	2003	16 043	87-06-19	15:35:46	201.8	−18.4	74.2	31.5
101	2006	8 116	87-06-20	09:56:58	86.3	−3.4	104.1	−5.0
102	2008	6 085	87-06-23	13:48:29	185.7	−16.0	68.7	37.3
103	2015	3 307	87-07-01	00:06:10	101.4	−66.5	263.9	−28.8
104	2018	14 441	87-07-03	12:11:15	253.7	−60.4	29.9	−23.9
105	2021	31 231	87-07-04	20:54:16	315.8	−18.7	90.7	−47.5
106	2032	19 344	87-07-11	14:39:25	68.8	−8.2	202.2	−21.9
107	2032	21 272	87-07-11	15:34:05	153.3	−51.0	136.3	−0.5
108	2035	35 258	87-07-14	20:53:39	14.5	−2.8	357.9	−53.8
109	2048	56 366	87-07-26	08:35:00	89.0	−26.1	98.5	−15.9
110	2051	37 819	87-07-28	23:12:33	41.8	−13.2	2.4	−46.0
111	2071	146 796	87-08-16	02:03:40	213.5	−12.2	272.6	32.1
112	2087	14 165	87-09-05	12:38:48	154.2	−9.3	164.3	38.2
113	2094	55 204	87-09-13	14:09:28	263.6	−18.1	90.1	−5.6
114	2099	562	87-09-15	23:19:26	291.2	−55.7	257.5	−40.9

TABLE I. (Continued).

	Run	Event	Date	Time	Azim. (deg)	Zeni. (deg)	R.A. (deg)	Decl. (deg)
115	2103	15 106	87-09-19	11:39:10	334.8	−44.6	67.2	−67.9
116	2105	23 494	87-09-24	14:35:23	205.7	−67.0	168.9	−15.2
117	2106	42 185	87-09-25	20:57:57	162.5	−31.9	291.7	19.7
118	2110	15 649	87-09-30	05:30:58	167.6	−4.9	66.8	47.1
119	2114	5 312	87-10-03	06:54:24	302.3	−14.2	334.7	−34.2
120	2120	86 992	87-10-10	21:39:54	265.9	−22.3	231.8	−9.9
121	2131	26 760	87-10-24	13:28:37	71.0	−44.6	249.4	−37.1
122	2138	62 292	87-10-30	11:42:52	44.9	−36.7	247.0	−54.3
123	2144	107 893	87-11-05	21:40:52	190.6	−10.4	313.0	42.1
124	2146	86 092	87-11-08	00:23:29	201.4	−54.7	357.7	−3.0
125	2156	89 777	87-11-15	02:48:28	170.9	−55.2	58.3	−1.9
126	2161	57 284	87-11-20	10:54:08	198.0	−36.1	164.7	15.5
127	2175	243 070	87-12-07	07:35:01	213.7	−8.0	104.1	35.5
128	2182	114 856	87-12-14	22:42:12	255.1	−44.9	335.6	−15.8
129	2185	47 060	87-12-17	11:05:41	55.0	−15.0	308.0	−36.8
130	2190	67 145	87-12-23	14:56:05	260.5	−21.6	205.8	−5.4
131	2203	1 033	88-01-09	02:04:05	240.9	−70.9	77.7	−25.6
132	2203	148 802	88-01-10	06:43:00	63.9	−14.4	260.6	−29.4
133	2205	3 962	88-01-13	02:22:18	145.4	−70.2	116.5	−19.5
134	2215	76 506	88-01-23	04:19:57	48.6	−4.8	257.5	−35.5
135	2217	32 885	88-01-26	05:12:53	19.3	−3.9	307.2	−52.9
136	2230	28 518	88-02-05	12:17:48	271.8	−49.6	229.4	−27.9
137	2241	122 500	88-02-17	23:48:41	312.3	−19.7	3.1	−45.2
138	2242	34 402	88-02-18	08:02:08	292.6	−32.3	152.3	−35.3
139	2242	35 119	88-02-18	08:09:57	236.9	−10.9	167.1	18.6
140	2245	326 470	88-02-22	16:46:48	60.4	−41.5	65.1	−43.7
141	2247	71 226	88-02-24	18:46:16	138.6	−34.1	66.5	9.6
142	2249	65 209	88-02-26	17:37:34	0.8	−6.1	195.9	−59.7
143	2250	136 393	88-02-28	08:58:53	162.2	−28.6	266.3	22.8
144	2257	10 253	88-03-04	01:18:22	237.3	−20.1	85.1	11.8
145	2260	196 509	88-03-06	23:56:36	162.6	−47.2	133.1	5.0
146	2260	302 408	88-03-07	22:06:00	250.0	−5.0	20.9	12.8
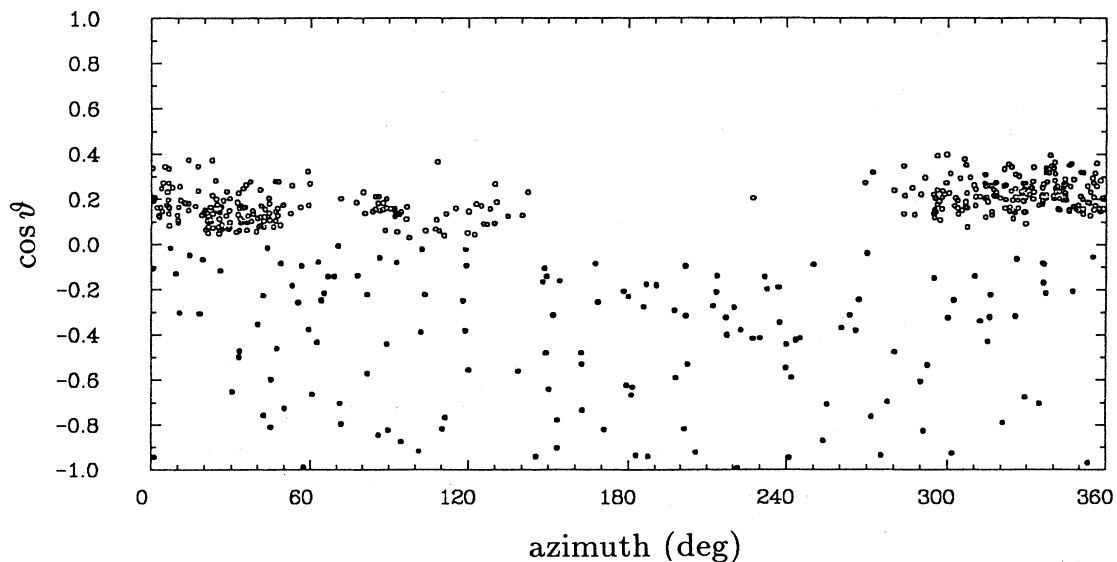
FIG. 2. Arrival direction of upward-going muons in the horizontal coordinate are shown by filled circles. Horizontal downward-going muons, which were selected by the off-line reduction and were judged as downward tracks by the eye scan, are also shown by empty circles. Most of horizontal downward-going muons are recorded from the south direction because of the thin rock overburden.
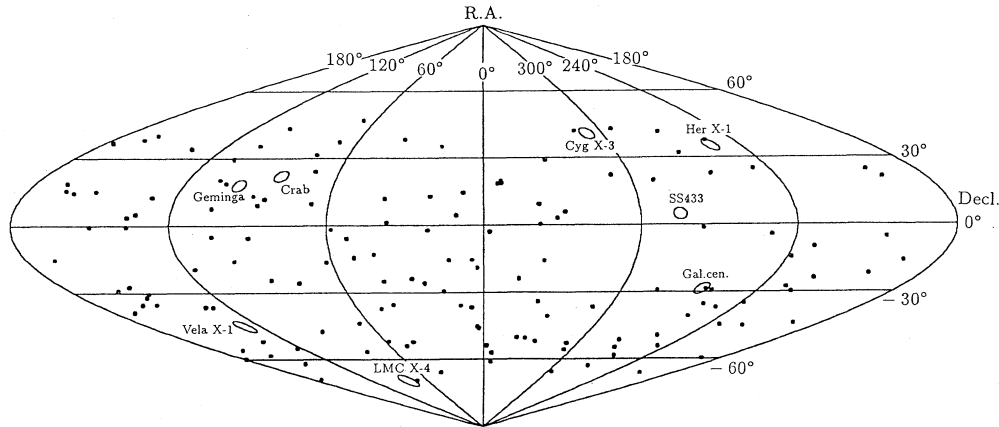
FIG. 3. Arrival direction of 146 upward-going muon events in the celestial coordinates. The 2.5° window around the celestial position of each object is also shown.

are well separated from downward-going muon background. A possible contamination by downward-going muons can be neglected.

To examine the directional correlation between muons and astronomical objects, the angular difference between the observed muons and the parent neutrinos has been carefully studied. This angular difference depends on the energy spectrum of neutrinos, which is not *a priori* known. The angular difference between the reconstructed muon and the parent neutrino, $\Delta\theta$, is written as

$$\Delta\theta = (\Delta\theta_1^2 + \Delta\theta_2^2 + \Delta\theta_3^2)^{1/2} , \qquad (2)$$

where $\Delta\theta_1$ is the error coming from manual reconstruction, $\Delta\theta_2$ is the scattering angle between the produced muon and parent neutrino, and $\Delta\theta_3$ is uncertainty in angle caused mainly by multiple Coulomb scattering of muon traveling the rock. $\Delta\theta_1$ is studied using Monte Carlo events and found to be 2.1°. This error is almost independent of position and angle of muon tracks in the detector. $\Delta\theta_2$ and $\Delta\theta_3$ depend on the energy spectrum

and the cutoff energies of parent neutrinos. $(\Delta\theta_2^2 + \Delta\theta_3^2)^{1/2}$ is calculated by a computer simulation for assumed cutoff energies E_c and spectral indices, i.e., the exponent γ of energy spectrum assumed as $E^{-\gamma}$, where E is the energy of the parent neutrino. The results of $\Delta\theta$ are 2.2° for $E_c = 10^{15}$ eV and $\gamma = 2.1$, and 3.5° for $E_c = 10^{12}$ eV and $\gamma = 2.7$. It is assumed in the following discussion that one standard deviation (68%) of upward-going muons comes from an angular window with a radius of 2.5°.

In Fig. 3 the arrival directions of 146 upward-going muons in celestial coordinates are plotted together with eight astronomical objects: Cygnus X-3, Hercules X-1, Crab nebula, Geminga, SS433, Galactic center, Vela X-1, and LMC X-4. Because the Kamiokande detector is located in the northern hemisphere, objects in the southern hemisphere sky are observable with higher efficiency. On the other hand, objects at larger declination ($\geq 53.6°$ N, i.e., 90° − Kamioka latitude) are not observable at all, because they are always above the horizon. Upward-going

TABLE II. The celestial position and distance from Earth of each astronomical object are listed in the second, third, and fourth columns. Exposure in m²yr, expected number of muons from atmospheric neutrino background, and observed upward-going muon events are presented in the fifth, sixth, and seventh columns, respectively. In the calculation of expected muon flux from the atmospheric neutrino background, the upward-going muon flux is obtained with assumption (i) (see text). The 90%-C.L. upper limit on upward-going muon flux from the direction of eight astronomical objects, the corresponding 90%-C.L. upper limit on the muon neutrino fluxes, and luminosities are also listed in the eighth, ninth, and tenth columns. The threshold energy of upward-going muons is 1.7 GeV. The cutoff energy and spectral index of parent neutrinos are assumed to be 10^{15} eV and 2.1, respectively.

Source	R.A. (deg)	Decl. (deg)	Distance (kpc)	Exposure (m²yr)	Expected background events	Observed events	90%-C.L. muon flux limit (cm⁻¹s⁻¹)	90%-C.L. neutrino flux limit (cm⁻²s⁻¹)	90%-C.L. neutrino luminosity limit (erg s⁻¹)
Cyg X-3	307.6	40.8	12	108.86	0.07	0	9.9×10^{-14}	16.8×10^{-6}	6.3×10^{39}
Her X-1	254.0	35.4	5	126.18	0.07	1	14.4×10^{-14}	24.5×10^{-6}	1.6×10^{39}
Crab	82.9	22.0	2	163.44	0.08	0	6.6×10^{-14}	12.2×10^{-6}	1.3×10^{38}
Geminga	97.7	17.8		170.34	0.08	0	6.3×10^{-14}	12.0×10^{-6}	
SS433	285.1	4.8	3	191.20	0.09	0	5.6×10^{-14}	9.6×10^{-6}	2.3×10^{38}
Gal. Cen.	265.5	−28.6	10	261.79	0.10	1	7.0×10^{-14}	11.8×10^{-6}	3.1×10^{39}
Vel X-1	128.4	−45.0	2	319.90	0.13	0	3.4×10^{-14}	7.8×10^{-6}	4.0×10^{37}
LMC X-4	81.0	−69.5	50	407.31	0.16	0	2.6×10^{-14}	5.4×10^{-6}	3.6×10^{40}

muons are uniformly distributed in proportion to the exposure of each celestial position. No candidate event was observed from the 2.5° radius window around six neutrino sources; one upward-going muon comes from the direction of Her X-1 and one from the Galactic center. The celestial position of astronomical objects, distance from Earth, exposure in units of m^2 yr, number of candidates from the window, and expected background from the window are listed in Table II. The number of observed events is consistent with the expected background and no significant signal is obtained. The total number from eight windows, 2, is also consistent with total expected background, 0.78. It should be noted that an angular window with a larger radius does not change the present result (see Fig. 3). The 90%-C.L. (-confidence-level) upper limits on the upward-going muon flux from eight astronomical objects are listed in Table II.

The corresponding 90%-C.L. upper limits on the muon-neutrino flux and on the muon-neutrino luminosity of each object are also calculated.[11] The probability $P(E)$ that a neutrino of energy E interacts in the rock outside the detector and produces a muon which passes through the detector is given in Ref. 12. $f(E)$ is defined as the probability that a neutrino of energy E coming from each object survives after passing through Earth. It can be calculated from column density of Earth in the direction of the object, and total cross section of the charged-current interaction for a given neutrino energy. The muon flux in the detector, Φ_μ, is given in terms of the neutrino spectrum $d\Phi_\nu/dE$ and the probabilities $P(E)$ and $f(E)$:

$$\Phi_\mu = \int_{E_{th}}^{E_c} P(E)f(E)\frac{d\Phi_\nu}{dE}dE , \qquad (3)$$

where E_c is the cutoff energy and E_{th} the minimum muon energy ($E_{th}=1.7$ GeV). If $d\Phi_\nu/dE$ is assumed to be $AE^{-\gamma}$, the numerical factor A can be calculated from Eq. (3). The neutrino flux Φ_ν is calculated by

$$\Phi_\nu = \int_{E_{th}}^{E_c} AE^{-\gamma}dE . \qquad (4)$$

The neutrino luminosity L ($E_{th} < E < E_c$) at each object is also obtained by the formula

$$L = 4\pi R^2 \int_{E_{th}}^{E_c} AE^{-\gamma}E\, dE . \qquad (5)$$

Assumed distances from Earth R are listed in Table II. The results of the calculations on the assumption that $E_c = 10^{15}$ eV and $\gamma = 2.1$ are presented in Table II. The fluxes and luminosities ($E_{th} < E < E_c$) are 16.8×10^{-6} $cm^{-2}s^{-1}$ and 6.3×10^{39} erg s^{-1} for Cygnus X-3, and 5.4×10^{-6} cm^{-2}s^{-1} and 3.6×10^{40} erg s^{-1} for LMC X-4.

These results should be compared with the expected fluxes and luminosities deduced from VHE and UHE γ-ray observations. The upward-going muon flux from Cygnus X-3 (Ref. 13) is expected to be $\sim 2 \times 10^{-15}$ cm^{-2}s^{-1}, whereas our 90%-C.L. upper limit is 9.9×10^{-14} cm^{-2}s^{-1}; one sees that the exposure is too small by 2 orders of magnitude. On the other hand, the observed flux limit for LMC X-4 is 2.6×10^{-14} cm^{-2} s^{-1} while the theoretical calculation[14] is $\sim 5 \times 10^{-14}$

cm^{-2}s^{-1}. Our observation already excludes the neutrino flux from LMC X-4 predicted by Ref. 14.

Since the Kamiokande detector is located at a lower latitude compared with the Irvine-Michigan-Brookhaven[15] (IMB) detector (41.7°N), our limits for objects in the northern hemisphere are more stringent than the IMB results. For example, our limit for Cygnus X-3 is lower than the IMB result (2.3×10^{-13} cm^{-2}s^{-1}) by a factor of more than 2. Note also that the Kamiokande observation is still background-free.

Because our observations have the potential ability to observe astronomical objects which have not been observed by photon emission, directional coincidences of upward-going muons in celestial coordinates are also examined to search for new astronomical objects. Numbers of muon pairs with angular separations less than 2°, 5°, and 10° are 4, 32, and 98, while expected numbers from a Monte Carlo study are 4.3, 26.7, and 98.9. They are consistent with random coincidences.

From the celestial position, right ascension of 353° and declination of 19°, three upward-going muons are observed within a 1° radius circle. The chance probability that three muons are observed within 2.1° radius circle is calculated, because this directional agreement is much better than the reconstruction error of Kamiokande, 2.1°. Expected upward-going muon events from this window are calculated to be 0.06. The probability that three events are observed, whereas the expected number is 0.06, is calculated by the Poisson distribution:

$$\frac{e^{-0.06}(0.06)^3}{3!} = 3.4 \times 10^{-5} . \qquad (6)$$

On the other hand, the number of circles with 2.1° radius within a total of 4π solid angle is

$$\frac{4\pi}{\pi\left[2.1 \times \frac{\pi}{180}\right]^2} = 3.0 \times 10^3 . \qquad (7)$$

By multiplying these two numbers, the probability that such a coincidence is observed in any celestial position is found to be 0.1. We cannot conclude that this is an observation of extraterrestrial high-energy neutrinos. A longer exposure as well as observation in other experiments are necessary.

III. UPWARD-GOING MUON FLUX AND A TEST OF NEUTRINO OSCILLATIONS

The upward-going muon flux is calculated from a total of 134 events which were taken in the weekday data. The upward-going muons from the low-efficiency directions recorded in the holiday runs would be amplified when the absolute flux is calculated because they are divided by the corresponding small efficiency. As a result, the total flux is affected by merely one or two such observed events. Therefore, the upward-going muons in the holiday data are not proper for the measurement of the flux and are not used here.

An average upward-going flux is obtained by

$$\Phi_{average} = \sum_j \frac{1}{\epsilon(\theta_j)S(\theta_j)} \Big/ 2\pi T , \qquad (8)$$
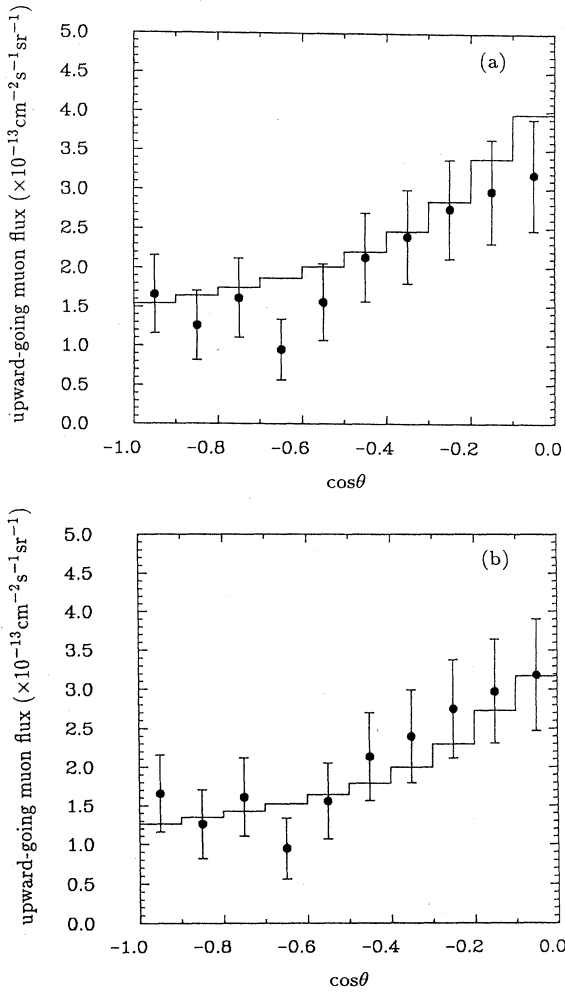
FIG. 4. Zenith-angle distribution of the upward-going muon flux observed in Kamiokande. The expected upward-going muon fluxes calculated with assumptions (i) and (ii) (see text) are also shown as the histograms (a) and (b), respectively.

where θ_j is the zenith angle of jth event, $S(\theta_j)$ and $\epsilon(\theta_j)$ are, respectively, the detection area and efficiency for upward-going muons with zenith angle θ_j. T is the total live time in weekday data-taking and 2π is the total solid angle corresponding to upward direction. The result of calculation is found to be $\Phi_{\text{average}} = (2.05 \pm 0.18) \times 10^{-13}$ cm^{-2}s^{-1}sr^{-1}.

The differential flux as a function of the cosine of the zenith angle, $(d\Phi_\mu/d\Omega)_{\text{expt}}$, is also calculated. Here, the 2π steradian solid angle is divided into 10 bins. The calculation procedure is the same as for the average flux; the only difference is that the summation is executed only for events in each zenith angle bin and that the element of solid angle is 0.2π. The result of this calculation with its statistical error is presented in Fig. 4.

To examine the neutrino oscillation hypothesis, this result should be compared with the expected flux of upward-going muons from atmospheric neutrinos. However, the calculation of the upward-going muon flux has a large uncertainty, and numerical results are assumption

dependent (see the Appendix for details). When we calculate the upward-going muon fux from possible oscillations, we use the following two sets of assumptions: (i) Volkova atmospheric neutrino flux,[16] Field-Feynman quark distribution,[17] and muon energy loss of the form $-dE_\mu/dX = a + bE$; (ii) Volkova atmospheric neutrino flux,[16] Eichten-Hinchliffe-Lane-Quigg (EHLQ) quark distribution,[18] and Lohmann muon energy loss.[19] We chose assumption (i) because it is the only published[20] result, and is widely approved. On the other hand, assumption (ii) is used because the numerical result is significantly different from (i) and other sets of assumptions would give results between these two extreme cases. Because Volkova[16] claims that the uncertainty of her calculation in absolute normalization is 20%, we take this number as an approximate uncertainty in the absolute normalization of the upward-going muon flux.

The upward-going muon flux adapted to the Kamiokande detector geometry is calculated to be 2.38×10^{-13} cm^{-2}s^{-1}sr^{-1} and 1.92×10^{-13} cm^{-2}s^{-1}sr^{-1} in cases (i) and (ii), respectively. Calculated zenith-angle distributions of the upward-going muon flux are shown in Figs. 4(a) and 4(b). Considering the absolute normalization error of 20%, the experimental flux obtained by Kamiokande is consistent with no neutrino oscillation.

Constraints on oscillation parameters Δm^2 and $\sin^2 2\theta$ are obtained in the following way. We analyze only $\nu_e \leftrightarrow \nu_\mu$ and $\nu_\mu \leftrightarrow \nu_\tau$ oscillations and do not consider oscillations among more than three species because neither our data nor the theoretical calculations have enough accuracy to fix more than two oscillation parameters. If Δm^2 and $\sin^2 2\theta$ are given, an oscillating neutrino flux can be calculated with Eq. (1) (in $\nu_\mu \leftrightarrow \nu_\tau$ oscillations) or with a differential equation for matter oscillations[7] (in $\nu_e \leftrightarrow \nu_\mu$ oscillations). By replacing the atmospheric neutrino flux with an oscillating atmospheric neutrino flux, the oscillating upward-going muon flux $(d\Phi_\mu/d\Omega)_{\text{osc}}$ can be obtained by the same method as the usual upward-going muon flux calculation. To compare the zenith-angle distributions of $(d\Phi_\mu/d\Omega)_{\text{expt}}$ and $(d\Phi_\mu/d\Omega)_{\text{osc}}$ the latter is also calculated for 10 zenith angle bins. In the following, $(d\Phi_\mu/d\Omega)^i_{\text{expt}}$ and $(d\Phi_\mu/d\Omega)^i_{\text{osc}}$ are used as the respective fluxes for the ith bin.

To evaluate the difference between $(d\Phi_\mu/d\Omega)^i_{\text{expt}}$ and $(d\Phi_\mu/d\Omega)^i_{\text{osc}}$ quantitatively, a χ^2 is defined as

$$\chi^2 = \min_\alpha \left[\sum_{i=1}^{10} \left[\frac{\left[\dfrac{d\Phi_\mu}{d\Omega} \right]^i_{\text{expt}} - \alpha \left[\dfrac{d\Phi_\mu}{d\Omega} \right]^i_{\text{osc}}}{\sigma_i} \right]^2 + \left[\frac{\alpha - 1}{\sigma_\alpha} \right]^2 \right], \quad (9)$$

where σ_i is the statistical error of $(d\Phi_\mu/d\Omega)^i_{\text{expt}}$ and α is the absolute normalization of $(d\Phi_\mu/d\Omega)^i_{\text{osc}}$. Because the nature of the uncertainty in the absolute normalization is unknown, it is supposed that α obeys a Gaussian distribution. σ_α is the one standard error of the absolute normalization, which is taken as 0.2.

For given Δm^2 and $\sin^2 2\theta$, the absolute normalization

α is adjusted so as to minimize χ^2. The minimum χ^2 (χ^2_{min}) in the Δm^2-$\sin^2 2\theta$ plane is searched for. Whether the given Δm^2, $\sin^2 2\theta$ are allowed or excluded is examined by evaluating the difference between χ^2 and χ^2_{min}. With χ^2 defined by Eq. (9), the region with

$$\chi^2(\Delta m^2, \sin^2 2\theta) \geq \chi^2_{min} + 4.6 \qquad (10)$$

is excluded with 90%-C.L. A detailed statistical discussion about this method is presented in Ref. 21. The 90%-C.L. excluded regions obtained by this method are shown in Fig. 5(a) for $\nu_e \leftrightarrow \nu_\mu$ and in Fig. 5(b) for $\nu_\mu \leftrightarrow \nu_\tau$ oscillations.

In $\nu_e \leftrightarrow \nu_\mu$ oscillation, no regions in Δm^2-$\sin^2 2\theta$ were excluded with 90%-C.L. when assumption (i) above is used. On the other hand, a small region is excluded with assumption (ii). This assumption dependence can be understood from the fact that the calculated flux with (ii) is considerably smaller than with (i). Our 90%-C.L. contour for $\nu_e \leftrightarrow \nu_\mu$ oscillation has already been excluded by previous reactor experiments,[22] and our result gives no new constraint on oscillation parameters. The reason our observation is relatively insensitive is explained as follows. Roughly speaking, if ν_e and ν_μ are well mixed with large oscillation parameters, the ν_μ flux would decrease to $\sim 70\%$ of its initial value. However, a $\sim 30\%$ defect cannot be detected easily because of the poor accuracy in the absolute flux normalization, which was taken as 20%. Further numerical study of the absolute normalization uncertainty might reduce the allowed region drastically.

In $\nu_\mu \leftrightarrow \nu_\tau$ oscillation, the present best limit on oscillation parameters was reported by the CERN-Dortmund-Heidelberg-Saclay-Warsaw (CDHSW) Collaboration.[23] Their excluded region with 90%-C.L. is $\Delta m^2 \geq 0.26$ eV^2 for maximum mixing and $\sin^2 2\theta \geq 0.053$ at $\Delta m^2 = 2.5$ eV^2. Although our experiment does not have good sensitivity in small $\sin^2 2\theta$ region, our 90%-C.L. limit for maximum mixing is $\Delta m^2 \leq 0.03$ eV^2 for assumption (i) and 0.0055 eV^2 for assumption (ii). Thus we obtain an excluded region in the Δm^2-$\sin^2 2\theta$ plot which is more than one order of magnitude larger than the previous region in the vicinity of large mixing angle. The neutrino-oscillation search using upward-going muons is likely to yield one of the most severe limits attainable in terrestrial experiments.

The IMB Collaboration[15] reported that their average upward-going flux is found to be $(2.41 \pm 0.21) \times 10^{-13}$ cm^{-2}s^{-1}sr^{-1}, whereas the expected flux is $(2.36 \pm 0.12 \pm 0.35) \times 10^{-13}$ cm^{-2}s^{-1}sr^{-1}. The error in the experimental result is the statistical error and the first and second errors in the expected flux are statistical and systematic errors, respectively. They claimed that the experimental result agrees well with the expectation. However, analysis based on neutrino oscillation is not presented in their paper.

In a previous paper,[10] we reported a deficit of contained muons in Kamiokande. Several physicists analyzed data and reported[24] that if $\nu_\mu \leftrightarrow \nu_\tau$ oscillation and the maximum mixing angle is assumed, a region $\Delta m^2 \gtrsim 10^{-3}$ eV^2 is favored. When the upward-going muon result obtained with assumption (ii) and the contained result are combined, the region $\Delta m^2 = 10^{-3}-10^{-2}$ eV^2 for large mixing remains allowed.

We summarize this section as follows. No significant constraint for oscillation parameters is obtained for $\nu_e \leftrightarrow \nu_\mu$ oscillations. On the other hand, if $\nu_\mu \leftrightarrow \nu_\tau$ vacuum oscillations and large mixing angle are assumed,
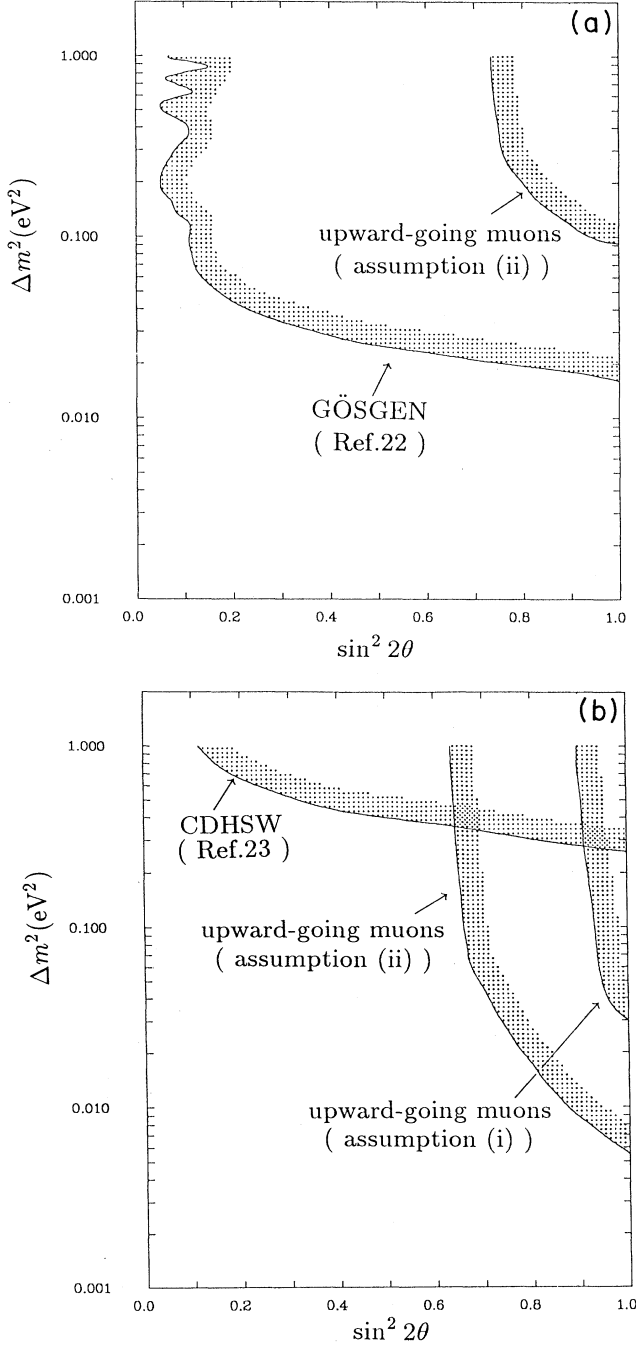
FIG. 5. The 90%-C.L. excluded regions in Δm^2-$\sin^2 2\theta$ plane are shown by shaded regions. Results from other experiments are also shown. (a) is for $\nu_e \leftrightarrow \nu_\mu$ oscillation and (b) is for $\nu_\mu \leftrightarrow \nu_\tau$ oscillation. The results from upward-going muon as 90%-C.L. contours with assumptions (i) and (ii) are drawn; when assumption (i) is used, no region is excluded for $\nu_e \leftrightarrow \nu_\mu$ oscillation.

$\Delta m^2 \gtrsim 10^{-2}$ eV^2 is newly rejected. If the deficits of contained muons are combined, $\Delta m^2 = 10^{-3} - 10^{-2}$ eV^2 with large mixing angle remains as a possible candidate for oscillation parameters.

IV. CONCLUSIONS

Upward-going muons produced in the surrounding rock by high-energy neutrinos from astronomical objects have been searched for using the large underground water Cherenkov detector, Kamiokande. During a total of 1255 days of observation, no significant signal was observed from the direction of eight astronomical objects. The 90%-confidence-level upper limits on upward-going muon flux with energy greater than 1.7 GeV are 9.9×10^{-14} cm^{-2}s^{-1} for Cygnus X-3, and 2.6×10^{-14} cm^{-2}s^{-1} for LMC X-4.

Our upward-going muon flux is compared with the calculation of the upward-going muon flux produced by the atmospheric neutrinos to examine the neutrino-oscillation hypothesis. The experimental average upward-going muon flux with energy greater than 1.7 GeV, $(2.05 \pm 0.18) \times 10^{-13}$ cm^{-2}s^{-1}sr^{-1}, is consistent with the calculated expectation with no oscillations. If $\nu_\mu \leftrightarrow \nu_\tau$ vacuum oscillations and large mixing angle are assumed, $\Delta m^2 \gtrsim 10^{-2}$ eV^2 is newly rejected. The 90%-C.L. upper limit on the Δm^2 for the maximum mixing is found to be $\Delta m^2 = 0.03$ and 0.0055 eV^2, depending on assumptions.

APPENDIX

In this appendix an uncertainty in the calculation of the expected upward-going muon flux is discussed.

The calculation of the upward-going muon flux consists of three physical processes. They are (1) atmospheric neutrino flux, (2) weak-interaction cross section between muon neutrino and rock, and (3) muon energy loss in the rock. Several numerical results are reported for each process.

The atmospheric neutrino flux has been calculated by many physicists. However, the energy range of the calculation is limited around the 1-GeV region because the purpose of the calculation is to understand background neutrino interactions against nucleon decays. The precise calculation up to the TeV region is presented only by Volkova[16] and Mitsui, Minorikawa, and Komori.[25] Both of their results are presented as tables of the $\nu_\mu + \bar\nu_\mu$ flux which are functions of the given neutrino energy and zenith angle. When two results are compared, one sees that the Volkova result is smaller by $\sim 10\%$ in the energy range 5–200 GeV. The discrepancy is larger than 20% for the horizontal direction.

The cross section of charged-current weak interactions is written by the usual weak interaction formula. The problem in the actual calculation is which quark distribution function should be used and what method of the approximation should be applied because the quark distribution function is a complex function of the invariant momentum transfer, $-Q^2$, and the Bjorken scaling variables. The parton-model approximation presented by Field and Feynman[17] is one of the traditional methods. However, Quigg, Reno, and Walker[12] claimed that the Q^2 independence of the quark distribution is broken at $E_\nu \sim 100$ GeV and the cross section becomes small in the higher-energy region. They suggested that the QCD evolution of the quark distribution function by EHLQ (Ref. 18) should be used in the higher-energy region. Actually, we confirmed that these results are in good agreement when the neutrino energy is small and that the discrepancy exceeds 10% in the energy region larger than 50 GeV.

For the muon energy loss in the rock, $-dE_\mu/dX = a + bE$ with $a = 2$ MeV/(g/cm^2) and $b = 3.9 \times 10^{-6}$ (g/cm^2)$^{-1}$ has been widely used. Recently, however, a precise computer calculation is reported by Lohmann, Kopp, and Voss[19] and they claimed that their energy loss is larger by several percent from the previous calculation at muon energy of 200 GeV.

The expected upward-going muon flux is affected by which programs presented above are used. Gaisser and Stanev[20] combined the Volkova neutrino flux, the Field-Feynman quark distribution function, and energy loss of the form $-dE_\mu/dX = a + bE$, and reported their result. To evaluate a systematic error in the flux calculation, we also calculated the flux for all of $2^3 = 8$ physical process combinations. Our result for the same program agrees well with their result and confirmed their calculation. Their calculation yields one of the largest fluxes among the eight assumptions. The smallest result of the eight assumptions is $\sim 80\%$ of the calculation of Gaisser and Stanev.

[1]D. Eichler, Nature (London) **275**, 725 (1978); V. S. Berezinsky, C. Castagnoli, and P. Galeotti, Nuovo Cimento **8C**, 185 (1985).

[2]V. S. Berezinsky and J. P. Ostriker, Astron. Astrophys. **66**, 325 (1978); H. Sato, Prog. Theor. Phys. **58**, 549 (1977).

[3]Y. Oyama *et al.*, Phys. Rev. Lett. **59**, 2604 (1987).

[4]S. Danaher *et al.*, Nature (London) **289**, 568 (1981); R. C. Ramb *et al.*, *ibid.* **296**, 543 (1982); M. Samorsky and W.

Stamm, Astrophys. J. **268**, L17 (1983); J. Lloyd-Evans *et al.*, Nature (London) **305**, 784 (1983); T. Kifune *et al.*, Astrophys. J. **301**, 230 (1986).

[5]R. J. Protheroe and R. W. Clay, Nature (London) **315**, 205 (1985).

[6]For a review of neutrino oscillations, see S. M. Bilenky and B. Pontecorvo, Phys. Rep. **41**, 225 (1978); A. K. Mann and H. Primakoff, Phys. Rev. D **15**, 655 (1977); D. Ayres *et al.*, *ibid.*

29, 902 (1984); S. M. Bilenky and S. T. Petcov, Rev. Mod. Phys. **59**, 671 (1987).

[7]L. Wolfenstein, Phys. Rev. D **17**, 2369 (1978); S. P. Mikheyev and A. Yu. Smirnov, Nuovo Cimento **9C**, 17 (1986).

[8]K. Arisaka et al., J. Phys. Soc. Jpn. **54**, 3213 (1985); Y. Oyama et al., Phys. Rev. Lett. **56**, 991 (1986).

[9]K. Hirata et al., Phys. Rev. Lett. **58**, 1490 (1987); W. Zhang et al., ibid. **61**, 385 (1988); K. S. Hirata et al., Phys. Rev. D **38**, 448 (1988).

[10]K. S. Hirata et al., Phys. Lett. B **205**, 416 (1988).

[11]M. Honda and M. Mori, Prog. Theor. Phys. **78**, 963 (1987).

[12]C. Quigg, M. H. Reno, and T. P. Walker, Phys. Rev. Lett. **57**, 774 (1986).

[13]T. K. Gaisser and T. Stanev, Phys. Rev. Lett. **54**, 2265 (1985); E. K. Kolb, M. S. Turner, and T. P. Walker, Phys. Rev. D **32**, 1145 (1985); **33**, 859(E) (1986).

[14]G. Cocconi, CERN Report No. 85-021, 1985 (unpublished).

[15]R. Svoboda et al., Astrophys. J. **315**, 420 (1987).

[16]L. V. Volkova, Yad. Fiz. **31**, 784 (1980) [Sov. J. Nucl. Phys. **31**, 1510 (1980)].

[17]R. Field and R. P. Feynman, Phys. Rev. D **15**, 1590 (1977).

[18]E. Eichten, I. Hinchliffe, K. Lane, and C. Quigg, Rev. Mod. Phys. **56**, 579 (1984); **58**, 1065(E) (1986).

[19]W. Lohmann, R. Kopp, and R. Voss, Report No. 85-03, 1985 (unpublished).

[20]T. K. Gaisser and T. Stanev, Phys. Rev. D **30**, 985 (1984).

[21]F. James, Comp. Phys. Commun. **20**, 29 (1980).

[22]K. Gabathuler et al., Phys. Lett. **134B**, 449 (1984).

[23]F. Dydak et al., Phys. Lett. **134B**, 281 (1984).

[24]J. G. Learned, S. Pakvasa, and T. J. Weiler, Phys. Lett. B **207**, 79 (1988); V. Barger and K. Whisnant, ibid. **209**, 365 (1988); K. Hidaka, M. Honda, and S. Midorikawa, Phys. Rev. Lett. **61**, 1537 (1988); a similar analysis by the Kamiokande Collaboration is now under study.

[25]K. Mitsui, Y. Minorikawa, and H. Komori, Nuovo Cimento **9C**, 995 (1986).